THE JOURNAL OF COMPARATIVE NEUROLOGY 455:531–546 (2003)

Connexin Immunoreactivity in Glial Cells of the Rat Retina

KATHLEEN R. ZAHS,[1*] PAULO KOFUJI,[2] CAROLA MEIER,[3] AND ROLF DERMIETZEL[3]

[1]Department of Physiology, University of Minnesota Medical School, Minneapolis, Minnesota 55455
[2]Department of Neuroscience, University of Minnesota Medical School, Minneapolis, Minnesota 55455
[3]Neuroanatomy and Molecular Brain Research, Ruhr Universität Bochum, 44780 Bochum, Germany

ABSTRACT

The rat retina contains two types of macroglial cells, Müller cells, radial glial cells that are the principal macroglial cells of vertebrate retinas, and astrocytes associated with the surface vasculature. In addition to the often-described gap-junctional coupling between astrocytes, coupling also occurs between astrocytes and Müller cells. Immunohistochemistry and confocal microscopy were used to identify connexins in the retinas of pigmented rats. Several antibodies directed against connexin43 stained astrocytes, identified using antibodies directed against glial fibrillary acidic protein (GFAP). In addition, two connexin43 antibodies stained Müller cells, identified with antibodies directed against S100 or glutamine synthetase. Connexin30-immunoreactive puncta were confined to the vitreal surface of the retina and colocalized with GFAP-immunoreactive astrocyte processes. Connexin45 immunoreactivity was associated with both astrocytes and Müller cells. We conclude that retinal glial cells express multiple connexins, and the patterns of immunostaining that we observe in this study are consistent with the expression of connexins30, -43, and possibly -45 by astrocytes and the expression of connexins43 and -45 by Müller cells. As gap-junction channels may be formed by both homotypic and heterotypic hemichannels, and the hemichannels may themselves be homomeric or heteromeric, there exists a multitude of possible gap-junction channels that could underlie the homotypic coupling between retinal astrocytes and the heterotypic coupling between astrocytes and Müller cells. J. Comp. Neurol. 455:531–546, 2003.

Indexing terms: gap junction; immunohistochemistry; immunostaining; astrocyte; Müller cell

Gap junctions may underlie a dynamic and complex network for signaling between glial cells. In addition to the often-described gap-junctional coupling between astrocytes (Tani et al., 1973; Yamamoto et al., 1990b; Dermietzel et al., 1991; Giaume et al., 1991; Lee et al., 1994; Ransom, 1995), coupling has been observed between astrocytes and oligodendrocytes (Ransom and Kettenmann, 1990; Robinson et al., 1993; Ochalski et al., 1997) and between astrocytes and Müller glial cells in the retina (Robinson et al., 1993; Zahs and Newman, 1997). Gap-junction channels provide a direct route for the intercellular exchange of ions and small metabolites and have been proposed to have a role in K^+ buffering (Mobbs et al., 1988), exchange of glucose metabolites (Tabernero et al., 1996; Giaume et al., 1997), and propagation of intercellular Ca^{2+} waves (Charles et al., 1992, 1993).

Each gap-junction channel is formed by the docking of two hemichannels, contributed by each cell of the coupled pair. These hemichannels, or "connexons," are hexamers composed of members of the connexin family of proteins (Beyer et al., 1987, 1990). Fifteen connexins have been identified thus far in mammals (Güldenagel et al., 2000).

Grant sponsor: National Institute of Health; Grant number: EY10383.

*Correspondence to: Kathleen R. Zahs, Department of Physiology, 6-125 Jackson Hall, University of Minnesota Medical School, 321 Church St. S.E., Minneapolis, MN 55455. E-mail: zahsx001@tc.umn.edu

Received 20 June 2002; Accepted 11 October 2002.

DOI 10.1002/cne.10524

Published online the week of December 9, 2002 in Wiley InterScience (www.interscience.wiley.com).

Gap junctions thus constitute a family of channels that may vary in their selective permeabilities, voltage sensitivities, rectification properties, and modes of regulation (Mills and Massey, 1995; Kumar, 1999; Beyer et al., 2000; Dermietzel et al., 2000a; Nicholson et al., 2000; White and Bruzzone, 2000).

The retina is a particularly good model system for studying the nature and regulation of gap-junctional communication between glial cells in situ. Vascularized mammalian retinas contain two major classes of macroglial cells, astrocytes and Müller cells. Astrocytes are present at the vitreal surface of the retina, and their processes ramify mainly in two dimensions. Müller cells are radial glia that span the depth of the retina. Both cell types are easily identifiable and accessible for electrophysiological recording and imaging studies in acutely isolated retinas (Robinson et al., 1993; Clark and Mobbs, 1994; Zahs and Newman, 1997). Gap junctions between retinal astrocytes and between astrocytes and Müller cells have been demonstrated through the intercellular spread of gap junction-permeant tracers. Gap junctions between astrocytes are permeable to both the fluorescent tracer Lucifer yellow and the biotin derivatives neurobiotin and biocytin, whereas the gap junctions between astrocytes and Müller cells are permeable primarily (rabbit, Robinson et al., 1993) or exclusively (rat, Zahs and Newman, 1997) to the biotin derivatives. Furthermore, in both species, tracer has been observed to spread only in the direction of astrocyte to Müller cell (Robinson et al., 1993; Zahs and Newman, 1997).

The apparent asymmetry of the coupling between retinal astrocytes and Müller cells could arise if the hemichannels contributed by astrocytes and Müller cells are formed by different connexins (Flagg-Newton and Loewenstein, 1980). The present study was undertaken to determine which connexins are present in retinal glia. Immunostaining coupled with confocal microscopy was used to identify several connexin proteins in the rat retina. Connexin43 (Cx43), connexin30 (Cx30), and connexin45 (Cx45) immunoreactivities were found to colocalize with astrocyte processes at the retinal surface. An antibody that recognizes Cx43 only when serine 368 is not phosphorylated (Nagy et al., 1997; Cruciani and Mikalsen, 1999) was found to stain Müller cells, and Cx45 immunoreactivity was observed to colocalize with Müller cell markers throughout the depth of the retina.

MATERIALS AND METHODS

Preparation of isolated retinas

Male Long-Evans rats (250–400 g) were deeply anesthetized with sodium pentobarbital (150 mg/kg) injected intraperitoneally. Animals were then trascardially perfused with oxygenated Ringer's solution, composed of (mM): KCl (2.5), NaCl (140), $CaCl_2$ (3), $MgCl_2$ (0.5), N-(2-hydroxyethyl)piperazine-N′-(2-ethanesulfonic acid) (5), dextrose (15), pH 7.4. Eyes were enucleated and the retinas dissected into oxygenated Ringer's solution. Retinas were incubated for 10 minutes at room temperature (approximately 24°C) in a mixture of collagenase-dispase (2 mg/ml; Boehringer-Mannheim, Indianapolis, IN) and DNAase (0.1 mg/ml; Sigma, St. Louis, MO) to facilitate removal of the vitreous. Isolated retinas were then fixed using one of three protocols. 1) For paraformaldehyde fixation, retinas were immersed overnight in 4% paraformaldehyde in 0.1 M phosphate buffer, pH 7.4, at 4°C, then rinsed extensively in phosphate-buffered saline, pH 7.4 (PBS), at room temperature. This duration of fixation was necessary to maintain the integrity of the tissue in the enzyme-treated whole mounts. 2) For ethanol fixation, retinas were immersed for 1 hour in 95% ethanol at 4°C, then rehydrated in a descending series of alcohols (70% ethanol, then 50% ethanol, then PBS, for 5 min each, at room temperature), followed by extensive rinses in PBS. 3) For ethanol-acetic acid fixation, retinas were fixed for 1 hour in 5% acetic acid in 95% ethanol at 4°C, then rinsed extensively in PBS. After fixation, each retina was cut into four pieces, to yield eight samples per animal.

In situ fixation

Rats were anesthetized and transcardially perfused with Ringer's solution as described above. One eye was removed and the retina isolated as described, while the rat continued to be perfused with 4% paraformaldehyde in 0.1 M phosphate buffer, pH 7.4. The second eye was then removed from the animal, and the retina was dissected into PBS, then postfixed overnight in 4% paraformaldehyde in 0.1 M phosphate buffer, pH 7.4, at 4°C. We were thus able to compare the pattern of immunostaining in the retina fixed in situ with the pattern of immunostaining in the paraformaldehyde-fixed, isolated retina from the same animal.

Immunostaining of retinal whole mounts

Immunostaining was carried out on retinal whole mounts. A variety of fixation protocols was tested for each antibody. After fixation and rinsing, retinas were incubated for 2 hour at room temperature with 10% normal serum (diluted in PBS with 1% Triton X-100) from the host species for the secondary antibodies to block nonspecific binding sites. The blocking solution was then removed and replaced with primary antibodies diluted in phosphate buffer with 1% thimerosal, 0.01% anti-foam A (Sigma; A5633), 5% powdered milk, and 0.3% Triton X-100, and the retinas were incubated for 3 days at 4°C on a shaking table. Retinas were then rinsed extensively in PBS and incubated with fluorescently conjugated secondary antibodies (diluted in PBS with 0.3% Triton X-100) for 3 days at 4°C on a shaking table. The secondary antibody solution was removed, and retinas were rinsed extensively with PBS, mounted, and coverslipped with Vectashield mounting medium (Vector Laboratories, Burlingame, CA) to retard fading of the fluorophores.

Immunostaining was conducted using a panel of antibodies directed against specific connexins. These antibodies are listed in Table 1. Most retinas were doubly immunostained with an anti-connexin antibody and an antibody directed against one of the following glial cell markers: glial fibrillary acidic protein (GFAP), to label retinal astrocytes (mouse anti-GFAP, Chemicon, Temecula, CA, MAB360, diluted 1:400; or rabbit anti-GFAP, Chemicon AB5040, diluted 1:50); glutamine synthetase (GS), to label Müller cells (mouse anti-GS, Chemicon MAB302, diluted 1:200; or goat anti-GS, Santa Cruz Biotechnology, Santa Cruz, CA, C-20, diluted 1:200); or S100, to label both astrocytes and Müller cells (rabbit anti-S100 [ββ homodimer], Dako, Carpinteria, CA, Z0311, 10 μg/ml; or mouse anti-S100, Chemicon, MAB079-1, 10 μg/ml). Secondary antibodies were obtained from Jackson Immunore-

TABLE 1. Anti-Connexin Antibodies Used in This Study[1]

	Species and immunogen	Antibody format and host	Fixation	Concentration
Connexin26				
Zymed 71-0500[2]	Rat Segment of cytoplasmic loop	Polyclonal, affinity purified Rabbit	ETOH	10 μg/ml
Zymed 13-8100	Rat Segment of cytoplasmic loop	Monoclonal Mouse	Unsuccessful; PF, ETOH, ETOH/Ac	10 μg/ml
Connexin30				
Zymed 71-2200	Mouse Unique portion of C-terminal	Polyclonal, affinity purified Rabbit	ETOH, PF	1–10 μg/ml
Connexin32				
Zymed 71-0600, lot 80642436	Rat Portion of cytoplasmic loop	Polyclonal, affinity purified Rabbit	PF	1–10 μg/ml
Chemicon MAB3069	Rat Isolated gap junctions[3]	Monoclonal Mouse	PF	1–10 μg/ml
Zymed 13-8200	Rat Segment of cytoplasmic loop	Monoclonal Mouse	Unsuccessful: PF, ETOH, ETOH/Ac	10 μg/ml
Connexin43				
Zymed 71-0700, lot 50826441, lot 80140147	Rat Portion of C-terminal	Polyclonal, affinity purified Rabbit	ETOH, PF	1–10 μg/ml
Zymed 71-0700, lot 90647439	Rat Portion of C-terminal	Polyclonal, affinity purified Rabbit	PF	1–10 μg/ml
KAαCx43	Rat	Polyclonal, affinity purified Rabbit	ETOH, PF	1:200
Zymed 13-8300	Rat Amino acids 360–376[4]	Monoclonal Mouse	ETOH, PF	1–10 μg/ml
Chemicon MAB3068	Rat Amino acids 252–270	Monoclonal Mouse	PF	10 μg/ml
Connexin45				
Chemicon AB1742[5]	Mouse C-terminal amino acids 285–298	Polyclonal, affinity purified Rabbit	ETOH, PF	10–25 μg/ml
Chemicon AB1745	Human Amino acids 354–367	Antiserum Rabbit	ETOH, PF	2.5–7.5 μg/ml
Chemicon MAB3100	Human Amino acids 354–367	Monoclonal Mouse	ETOH, PF	1–10 μg/ml
Chemicon MAB3101	Human Amino acids 354–367	Monoclonal Mouse	ETOH, PF	1–10 μg/ml

[1]PF, fixation with 4% paraformaldehyde in 0.1 M phosphate buffer; ETOH, fixation with ethanol; ETOH/AC, fixation with ethanol/acetic acid; for details see *Materials and Methods.*
[2]Demonstrated cross-reactivity with connexin30 (Nagy et al., 1999).
[3]Manufacturer claims antibody is probably directed against an epitope located between amino acids 95 and 125.
[4]Reported to recognize Cx43 only when unphosphorylated at serine 368 (Nagy et al., 1997; Cruciani and Mikelsen, 1999).
[5]Demonstrated cross-reactivity with connexin43 (Coppen et al., 1998).

search (West Grove, PA) and used at 7 μg/ml. For double-labeling experiments, one secondary antibody was conjugated to fluorescein isothiocyanate (FITC) and the other to Cy3 or Texas red.

The control used for each antibody was determined by the availability of reagents. Ideally, retinal tissue from animals with targeted deletions of the genes encoding each connexin would be used as controls for the specificity of affinity-purified antibodies in the retina (Meier et al., 2002). In the current study, immunostaining was performed on retinas from mice with a targeted deletion of the gene for Cx32 (Nelles et al., 1996). Cx30-deficient animals do not yet exist, Cx45-deficient embryos die in utero (Kumai et al., 2000), and Cx43-deficient animals die at birth (Reaume et al., 1995), so we relied on peptide preabsorption (when peptide antigen or its sequence was available from the manufacturer; see Table 2) and Western blotting to confirm the specificity of the antibodies directed against these connexins. For peptide preabsorption controls, primary antibodies were incubated for 2–4 hours at room temperature with an excess of the peptide against which the antibody was generated, prior to addition to the tissue. Control peptides were obtained from the manufacturer of each antibody, with the exception of the peptide used to preabsorb the Chemicon MAB3101 (mouse anti-human Cx45). This peptide was generated by SigmaGenosys (The Woodlands, TX) using the amino acid sequence provided by Chemicon. Additional controls consisted of incubation with diluent from which the primary antibody was eliminated. Control samples were derived from the same retinas as the corresponding experimental samples. For each antibody, immunostaining was performed on at least three samples obtained from different animals on different days.

Retinal sections

Two of the antibodies (Zymed 13-8300, monocolonal anti-Cx43; Chemicon MAB3101, monoclonal anti-Cx45) were also tested on cryosections of retina. Lethal injections of sodium pentobarbital were administered to two rats, and the eyes were enucleated and immersion fixed for 4 hours in 4% paraformaldehyde in 0.1 M PB at 4°C. The eyes were then rinsed three times in PBS, the cornea and lens were removed, and the resulting eyecups were cryoprotected in 30% sucrose in PB and embedded in a mixture of OCT compound (Miles Scientific, Naperville, IL) and Aqua-Mount (Lerner Laboratories, Pittsburgh, PA) (Jones et al., 1986). Twelve-micrometer-thick sections were cut on a cryostat.

Sections were doubly immunostained using Dako rabbit anti-S100 (10 μg/ml) and either mouse anti-Cx43 (Zymed 13-8300, 5 μg/ml) or mouse anti-Cx45 (Chemicon MAB3101, 5 μg/ml). Sections were gently rinsed four times with PBS, then incubated for 1 hour at room temperature with 10% normal donkey serum diluted in PBS with 1% Triton X-100. This blocking solution was then removed, and the sections were incubated for 16 hours at 4°C with primary antibodies diluted in the same buffer as was used for the retinal whole mounts. Retinas were then rinsed four times with PBS and incubated with fluores-

TABLE 2. Summary of Results

	Immunohistochemistry	Control
Connexin26		
Zymed 71-0500[1]	Dffuse staining of astrocyte processes	Staining eliminated by peptide preabsorption (5× peptide)[2]
Zymed 13-8100	No staining	
Connexin30		
Zymed 71-2200	Punctate, colocalizes with astrocyte processes	Staining eliminated by peptide preabsorption (5× peptide)
Connexin32		
Zymed 71-0600	*Nonspecific* staining of Müller cells and neurons	Staining also observed in retinas of Cx32 null mice
Chemicon MAB3069	*Nonspecific* staining of Müller cells and neurons	Staining also observed in retinas of Cx32 null mice
Zymed 13-8200	No staining	
Connexin43		
Zymed 71-0700, lot 50826441	Punctate, colocalizes with astrocyte processes	Staining eliminated by peptide preabsorption (5× peptide)
Zymed 71-0700, lot 80140147	Punctate, colocalizes with astrocyte processes	Staining eliminated by peptide preabsorption (5× peptide)
Zymed 71-0700, lot 90647439	Punctate, colocalizes with astrocyte processes and Müller cells	Staining eliminated by peptide preabsorption (5× peptide)
KAαCx43	Punctate, colocalizes with astrocyte processes	No primary antibody
Zymed 13-8300	PF flx:Punctate, colocalizes with Müller cells ETOH flx: diffuse, colocalizes with Müller cells	Staining eliminated by peptide preabsorption (5× peptide)
Chemicon MAB3068	Punctate, colocalizes with astrocyte processes	No primary antibody
Connexin45		
Chemicon AB1742[3]	Punctate, colocalizes with Müller cells and horizontal cells	Staining eliminated by peptide preabsorption (5× peptide)
Chemicon AB1745	Punctate, colocalizes with Müller cells and horizontal cells	Staining reduced by peptide preabsorption (10× peptide)
Chemicon MAB3100	Dendrites in IPL; possibly Müller cells; inconsistent	No primary antibody
Chemicon MAB3101	Müller cells; astrocytes; possibly dendrites in IPL	Staining eliminated by peptide preabsorption (5× peptide)

[1]Demonstrated cross-reactivity with connexin30 (Nagy et al., 1999).
[2]Concentration of peptides (weight/volume) expressed relative to concentrations of antibodies.
[3]Demonstrated cross-reactivity with connexin43 (Coppen et al., 1998).

cently conjugated secondary antibodies (FITC-donkey anti-mouse and Texas red-donkey anti-rabbit, each 7 μg/ml, diluted in PBS with 0.3% Triton X-100) for 4 hours at room temperature. The secondary antibody solution was removed, and retinas were rinsed with PBS and coverslipped with Vectashield. Control sections were exposed to anti-connexin antibodies preincubated with peptide antigen (25 μg/ml), as described for the retinal whole mounts.

Confocal microscopy

Immunostained retinas were imaged with a Leica TSM laser scanning confocal microscope. For a detailed examination of the staining pattern in particular layers of the retina, retinal whole mounts were used. Optical sections parallel to the retinal surface were collected using a 100× oil-immersion objective. Five to twenty serial confocal images were collected at 0.2 μm intervals within each retinal layer. When collected as 512 pixel × 512 pixel, eight-bit grayscale images, these images had a resolution of 0.2 μm/pixel. As a result of variations in antibody penetration and light scattering, the intensities of the fluorescence signals obtained in each layer of the retinal whole mounts may not accurately reflect the relative amounts of antigens in each layer. Because it was not possible to make quantitative comparisons between layers, the settings for the laser and photomultiplier tubes (PMTs) were optimized for each retinal layer.

Retinal sections were scanned using a 50× oil-immersion objective. Images were collected as 512 pixel × 512 pixel, eight-bit gray-scale images, which resulted in a resolution of 0.4 μm/pixel. Images were collected at 0.4 μm intervals through the thickness of the section.

Simultaneous detection of FITC and Texas red or Cy3 was accomplished using 488 nm/568 nm excitation from an ArKr laser, with 530/30 nm bandpass (FITC) and 665 nm (Texas red) or 590 nm (Cy3) longpass emission filters. Control samples were scanned using the same settings for the laser and PMTs as were used to scan the corresponding experimental samples.

Image reconstruction

The figures presented in Results were created using Adobe Photoshop running on a PC, after confocal images were first processed using MetaMorph software (Universal Imaging, West Chester, PA). To illustrate the pattern of staining within a retinal layer, a series of confocal images spanning 1–2 μm was projected onto a single plane by assigning to each pixel in the projection the intensity of the brightest pixel at that X-Y location from among those in the stack of images. To illustrate the pattern of staining in the retinal sections, MetaMorph was similarly used to project stacks of confocal images (spanning 10 μm) onto a single plane. For side-by-side comparisons of immunostained retinas and their corresponding controls, the MetaMorph projections for the two samples were pasted into a single image within Photoshop, and adjustments to brightness and contrast were performed simultaneously on the two samples. It should be noted that, for the images depicting the staining within each retinal layer, the brightness and contrast were adjusted for each layer separately. These figures therefore do not reflect relative amounts of staining in those layers. However, the images of the retinal sections provide an accurate representation of the relative amounts of staining through the depth of the retina.

Western blotting

Male Long-Evans rats (250–400 g) were killed with an overdose of sodium pentobarbital (150 mg/kg) administered intraperitoneally. Retinas, brain (cerebral cortex), heart (ventricles), and liver were rapidly dissected, washed with PBS, and homogenized in sample buffer containing 320 mM sucrose, 0.2 mM phenylmethanesulfonyl fluoride, pepstatin A (1 μg/ml), leupeptin (1 μg/ml), and benzamide (100 μg/ml; all protease inhibitors from Sigma). Homogenates were centrifuged for 5 minutes at 2,000*g* (4°C) to remove insoluble material. The supernatant was then centrifuged at 100,000*g* (4°C) to obtain the crude membrane fraction, which was then washed once in the sample buffer. The protein concentration in the crude membrane fraction was determined using the Coomassie Plus Protein Assay Reagent Kit (Pierce, Rockford IL), following the manufacturer's instructions. Bovine serum albumin was used as the standard. Membranes were stored at −80°C.

Proteins in the membrane preparations from each tissue of interest were separated by sodium dodecyl sulfate-polyacrylamide gel electrophoresis (SDS-PAGE; 4–20% gradient gel; Invitrogen, Carlsbad, CA) under reducing conditions and electrophoretically transferred to a 0.2 μm polyvinylidene difluoride membrane (Invitrogen). Blots were incubated with 5% powdered milk in PBS with 0.2% Tween-20 for 1 hour at room temperature to block nonspecific binding of the antibodies. After they were rinsed in PBS, blots were incubated overnight at 4°C with primary antibody diluted in PBS/0.2% Tween-20/1% powdered milk. Primary antibodies were used at the following dilutions: rabbit anti-Cx30 (Zymed; 71-2200, lot 00460029, 1:1,000 = 0.5 μg/ml), rabbit anti-Cx43 (Zymed; 71-0700, lot 80140147, 1:1,000 = 0.5 μg/ml; and lot 90647439, 1:10,000 = 50 ng/ml), mouse anti-Cx43 (Zymed; 13-8300, 1:1,000 = 1 μg/ml), and mouse anti-Cx45 (Chemicon; MAB3101, 1:1,000 = 1 μg/ml). For peptide preabsorption controls, prior to addition to the blots, primary antibodies were incubated for 2–4 hours at room temperature with a 5× concentration (weight/volume) of the peptide against which the antibody was generated. After the primary antibody incubation, blots were rinsed for 3 × 15 min in PBS/0.2% Tween-20/5% powdered milk, then incubated with secondary antibody for 1 hour at room temperature (horseradish peroxidase-conjugated donkey anti-mouse 1:10,000 or donkey anti-rabbit 1:3,000; Jackson Immunoresearch; diluted in PBS/0.2% Tween-20/1% powdered milk). After being rinsed with PBS, blots were developed using a chemiluminescence method (ECL: Amersham, Piscataway, NJ; or LumiLight-Plus: Roche Diagnostics, Indianapolis, IN).

In some cases, after antibody incubation and development, blots were stripped of antibodies and reprobed. Blots were incubated in stripping buffer (100 mM 2-mercaptoethanol, 2% SDS, 62.5 mM Tris-HCl, pH 6.7) for 45 minutes at 70°C. Removal of the antibodies was confirmed by developing the exposed blots with chemiluminescence reagents. In all cases, there was no detectable signal after stripping, indicating that the secondary antibodies, at least, had been removed. Blots were rinsed for 3 × 10 min with PBS-Tween and then probed with another primary antibody.

RESULTS

The results obtained with the various anti-connexin antibodies are summarized in Table 2, and patterns of immunostaining are described in detail below.

Cx30

Cx30-immunoreactive (-IR) puncta colocalized with GFAP-IR astrocyte processes (see Fig. 2A,B). Although we did not subject the images to quantitative analysis, it was our impression that the Cx30 immunoreactivity was localized primarily on the distal processes of astrocytes, where they contacted blood vessels. There were no qualitative differences in staining between retinas fixed in situ and acutely isolated retinas. Peptide preabsorption eliminated staining with this antibody (not shown).

On Western blots, this antibody stained a band at approximately 30 kDa in membrane preparations from brain as well as a fainter band at approximately 50 kDa. A single band, at approximately 33–34 kDa, was stained in membrane preparations from the retina (Fig. 1D). The differences in electrophoretic mobility of the Cx30-IR bands from brain and retina might represent differences in posttranslational modification of Cx30 in the two tissues or even the differential expression of two Cx30 transcripts (Dahl et al., 1996).

Cx43

Four polyclonal and two monoclonal antibodies directed against Cx43 were used to stain retinal whole mounts. Four of the antibodies (Zymed 71-0700, lots 50826441 and 80140147; KAαCx43; Chemicon MAB3068) yielded discrete immunoreactive puncta that were located primarily within the nerve fiber layer at the vitreal surface of the retina. In retinas doubly immunostained with an antibody directed against GFAP, the Cx43-IR puncta were located along GFAP-IR astrocyte processes (Fig. 2C,D). Cx43-IR puncta in the retinal ganglion cell (RGC) layer and inner plexiform layer (IPL) were associated with the occasional astrocyte processes that descended into these layers. There were no qualitative differences in staining between retinas fixed in situ and acutely isolated retinas.

The Zymed monoclonal antibody (13-8300) directed against Cx43 yielded a very different pattern of staining. In ethanol-fixed tissue, diffuse staining of Müller cells was observed (not shown). In paraformaldehyde-fixed retinas, punctate immunoreactivity was present throughout the depth of the retina. This Cx43 immunoreactivity was localized to Müller cells, identified in retinas doubly labeled with 13-8300 and antibodies directed against either S100 or glutamine synthetase. In the sample illustrated in Figure 3, a polyclonal anti-S100 labeled both astrocytes and Müller cell endfeet at the vitreal surface of the retina. Cx43 immunoreactivity was observed primarily over the Müller cells, distinguishable from the astrocytes by their fainter labeling with the anti-S100. Within the RGC layer, immunoreactive puncta were observed in S100-IR Müller cell processes, located between neuronal somata. Punctate Cx43 immunoreactivity was observed throughout the inner plexiform layer. Within the IPL, the proximal stalks of Müller cells that traverse this layer were strongly immunoreactive for S100. However, there was also fainter, more diffuse S100 immunoreactivity that may represent the fine side branches of Müller cells that wrap the synapses in the IPL (Newman and Reichenbach, 1996). Since S100 may be secreted by glial cells, it is also possible that some of the diffuse S100 immunoreactivity was extracellular (Shashoua et al., 1984; Van Eldik and Zimmer, 1987). In the inner portion of the inner nuclear layer (INL), punctate staining was observed in S100-IR profiles located between unstained neuronal somata. Within the middle portion of the INL, Cx43 immunoreactivity was observed primarily over S100-IR Müller cell processes, although occasionally Cx43-IR puncta were observed at the borders between S100-IR Müller cell somata. Because it was not possible to distinguish individual Müller cell processes in these samples, we were unable to determine whether Cx43 immunoreactivity occurred within or between pro-

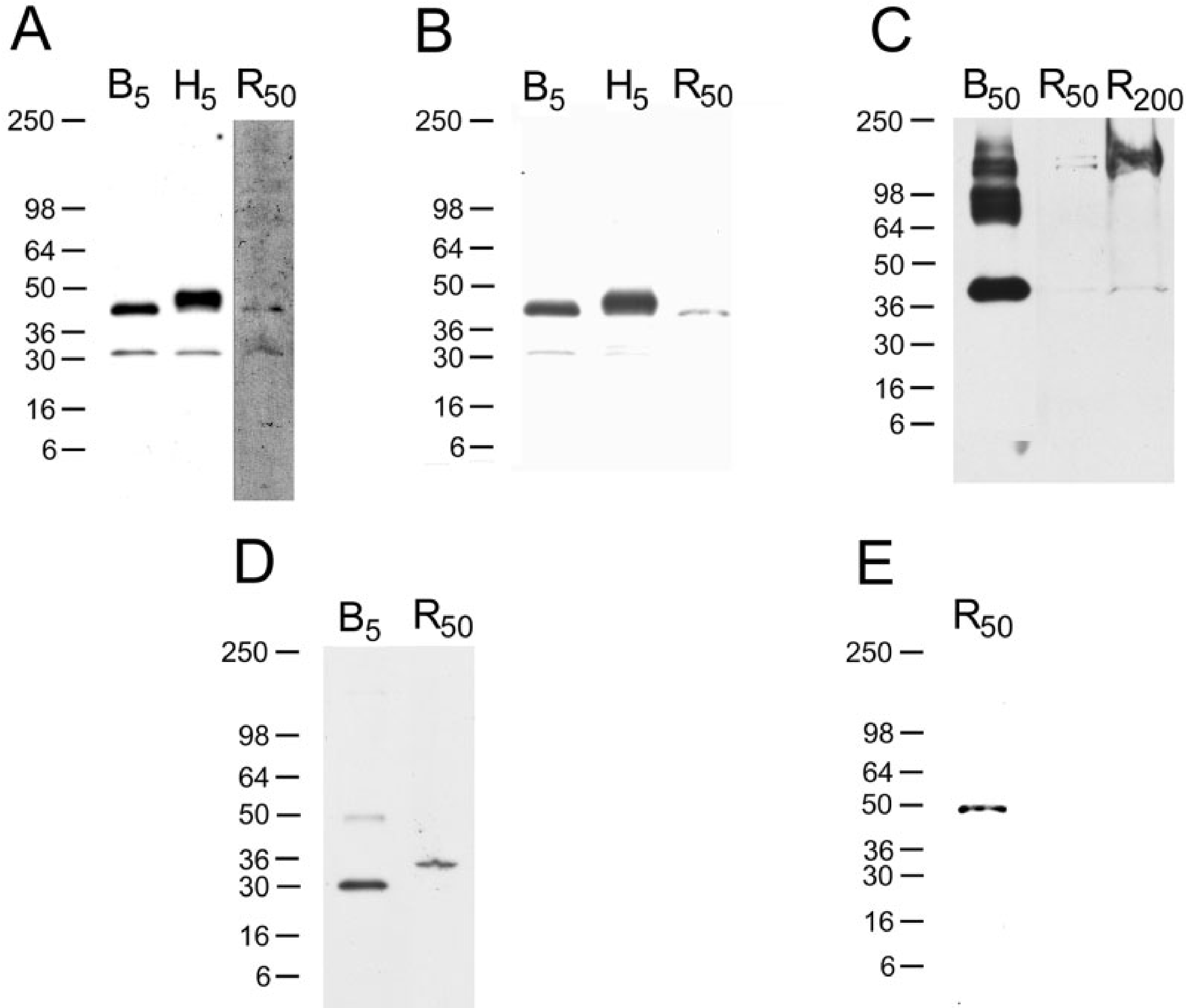

Fig. 1. Western blots. Proteins in the membrane preparations from each tissue of interest were separated by SDS-PAGE under reducing conditions, transferred to PVDF membranes, and probed with various anti-connexin antibodies, as described in Materials and Methods. **A:** Polyclonal rabbit anti-rat Cx43 (Zymed 71-0700, lot 80140147). Because of the large difference in the intensity of bands from brain and heart compared with retina, the lanes from brain and heart are shown from a film exposed for a shorter period than the film used to show the bands in retina. **B:** Polyclonal rabbit anti-rat Cx43 (Zymed 71-0700, lot 90647439). **C:** Monoclonal mouse anti-rat Cx43 (Zymed 13-8300). **D:** Polyclonal rabbit anti-mouse Cx30 (Zymed 71-2200, lot 00460029). **E:** Monoclonal mouse anti-human Cx45 (Chemicon MAB3101). Positions of molecular weight markers are shown to the left of each blot. B, brain (cerebral cortex); H, heart (ventricles); R, retina; subscripts indicate amount of protein (in micrograms) loaded in each lane.

cesses. This pattern persisted in the outer portion of the INL. While Cx43-IR puncta were observed in the outer plexiform layer, we could not clearly distinguish the processes of Müller cells in this layer. Within the outer nuclear layer (ONL), S100-IR Müller cell processes surrounded the photoreceptor cell bodies, and Cx43-IR profiles were again located over these Müller cell processes. In retinas doubly labeled with 13-8300 and antibodies directed against GFAP, some Cx43-IR puncta were located along astrocyte processes, although the majority of the Cx43 immunoreactivity at the retinal surface did not colocalize with astrocytes (Fig. 2G). There were no qualitative differences in staining between retinas fixed in situ and acutely isolated retinas. Peptide preabsorption eliminated staining with this antibody.

In radial sections of the retina (Fig. 3G–K), antibody 13-8300 strongly labeled the endfeet and the proximal stalks of Müller cells. Additional Cx43 immunoreactivity was associated with S100-IR Müller cell somata and processes throughout the depth of the retina, consistent with the pattern of staining seen in the retinal whole mounts.

Finally, a third lot of the polyclonal Zymed 71-0700 (lot 90647439) yielded punctate immunoreactivity throughout the depth of the retina. At the retinal surfaces, this Cx43 immunoreactivity colocalized with GFAP-IR astrocyte processes (Fig. 2D). In other retinal layers, Cx43 immunoreactivity was localized to Müller cells, identified with either anti-S100 or anti-glutamine synthetase (not shown), and appeared very similar to the immunoreactivity observed with the Zymed 13-8300.

Western blots were used to assess the specificity of the antibodies that gave the most robust staining. Although they produced different patterns of immunostaining in retinal whole mounts, the two polyclonal antibodies tested (Zymed 71-0700, lots 80140147 and 90647439) yielded similar results on Western blots (Fig. 1A,B). In brain and retina, both antibodies detected bands at approximately 43 kDa and approximately 32 kDa. The latter band may represent a Cx43 proteolysis product; bands of similar size have been reported in Western blots of brain and retina (Giblin and Christensen, 1997) and heart (Manjunath et al., 1987; Hofer and Dermietzel, 1998) with the use of other anti-Cx43 antibodies. Similar bands were detected in blots from heart, except that, in the heart, these antibodies detected at least a doublet at approximately 43 kDa. Such doublets, and even triplets, are commonly detected by anti-Cx43 antibodies in blots from heart and represent the presence of (multiply) phosphorylated forms of Cx43 (Musil and Goodenough, 1991; Laird et al., 1991). The absence of the bands representing the (multiply) phosphorylated forms of Cx43 in samples from retina and brain may be due to a greater susceptibility of Cx43 to post-mortem dephosphorylation in neural tissues than in heart in our preparations (Hossain et al., 1994b). The monocolonal anti-Cx43 (Zymed 13-8300) stained a band at approximately 43 kDa in samples from brain and retina as well as higher molecular weight species that may represent connexin multimers (Fig. 1C). This antibody has been reported to recognize Cx43 only when serine 368 is not phosphorylated (Nagy et al., 1997; Cruciani and Mikalsen, 1999).

Cx32

Two antibodies directed against Cx32 (Zymed polyclonal antibody 71-0600 and Chemicon monoclonal antibody MAB3069) yielded punctate staining throughout the depth of the retina (not shown). However, because these antibodies yielded a pattern of immunostaining in retinas from Cx32-null mice that was indistinguishable from that in rat retinas, it was concluded that these antibodies do *not* specifically immunostain Cx32 in the retina.

Cx45

Initial experiments using a polyclonal antibody directed against Cx45 (Chemicon AB1742) yielded punctate staining throughout the depth of the retina, and the Cx-IR puncta largely colocalized with Müller cell markers (not shown). Preabsorption with the synthetic peptide used to generate this antibody eliminated this staining. However, this antibody was subsequently shown to cross-react with Cx43 (Coppen et al., 1998). Later experiments using a second polyclonal antiserum (Chemicon AB1745) generated against a synthetic peptide corresponding to amino acids 354–367 of human Cx45, which does not possess sequence homology with Cx43 (Coppen et al., 1998), yielded a similar pattern of staining: immunoreactive puncta were observed throughout the depth of the retina, and these Cx45-IR puncta were primarily associated with Müller cells identified using either anti-S100 or anti-glutamine synthetase (not shown). Peptide preabsorption greatly reduced, but did not completely eliminate, staining with this antibody. Finally, punctate immunoreactivity that largely colocalized with Müller cell markers was obtained with a monoclonal antibody (Chemicon MAB3101) directed against amino acids 354–367 of human Cx45 (Fig. 4). Pronounced Cx45 immunoreactivity was found in the inner retina. Cx45-IR puncta were observed over astrocytes at the vitreal surface in retinas doubly labeled with anti-S100 (Fig. 4A) and over Müller cell processes in the RGC layer (Fig. 4B). In the IPL, some Cx45 immunoreactivity occurred over the proximal stalks of Müller cells, identified by heavy S100 immunoreactivity. However, as with Cx43 immunoreactivity in the IPL, it was not possible to determine whether the majority of Cx45-IR profiles in this layer was associated with the fine processes of Müller cells. In the middle of the INL, Cx45-IR puncta were located over S00-IR Müller cell somata and processes (Fig. 4D). In addition, linear arrays of immunoreactive puncta in the innermost region of the INL may represent staining of neuronal processes (Fig. 4C). At the outer border of the INL (Figs. 4E, 5), Cx45 immunoreactivity occurred over S100-IR Müller cell processes surrounding horizontal cells. Finally, Cx45 immunoreactivity occurred over Müller cell processes surrounding the somata of photoreceptors in the ONL (Fig. 4F). Peptide preabsorption eliminated staining with this antibody.

Staining of radial sections of the retina with MAB3101 confirmed the laminar distribution of connexin immunoreactivity observed in the whole mounts. However, the radial sections proved to be less favorable for determining the cellular localization of Cx45-IR puncta compared withthe optical sections taken parallel to the retinal layers. Cx45-IR puncta were located over S100-labeled Müller cell somata in the middle of the INL in radial sections, as in the whole mounts. Pronounced labeling was also seen in the inner part of the INL in sections, but it was not possible to distinguish between the labeling of Müller cell processes and the labeling of neurons. In radial sections, which more accurately reflect the relative intensity of staining in the different retinal layers than do the confocal images through whole mounts, the Cx45 immunoreactivity in the ONL was much weaker than in the other layers.

The monoclonal anti-Cx45 stained a single band at approximately 48 kDa in samples from retina (Fig. 1E). This antibody did not detect any bands on blots from brain (50 μg protein/lane). Peptide preabsorption eliminated staining of blots with this antibody. The AB1745 serum stained bands at approximately 48 kDa on blots of brain and retina, although this crude serum stained multiple additional bands on these blots (not shown).

Cx26

Cx26 has been demonstrated in ependymal cells (Dermietzel et al., 1989; Spray et al., 1991). Because the apical processes of Müller cells contact the subretinal space, a ventricular compartment, these cells have been characterized as ependymoglial cells (Reichenbach and Robinson, 1995). We therefore suspected that Müller cells might express Cx26. In initial experiments, we observed diffuse staining of astrocyte processes when using a polyclonal antibody directed against Cx26 (Zymed 71-0500), which has since been demonstrated to cross-react with Cx30 (Nagy et al., 1999). We failed to observe staining with the monoclonal anti-Cx26 (Zymed 13-8100) with any of the fixation protocols.

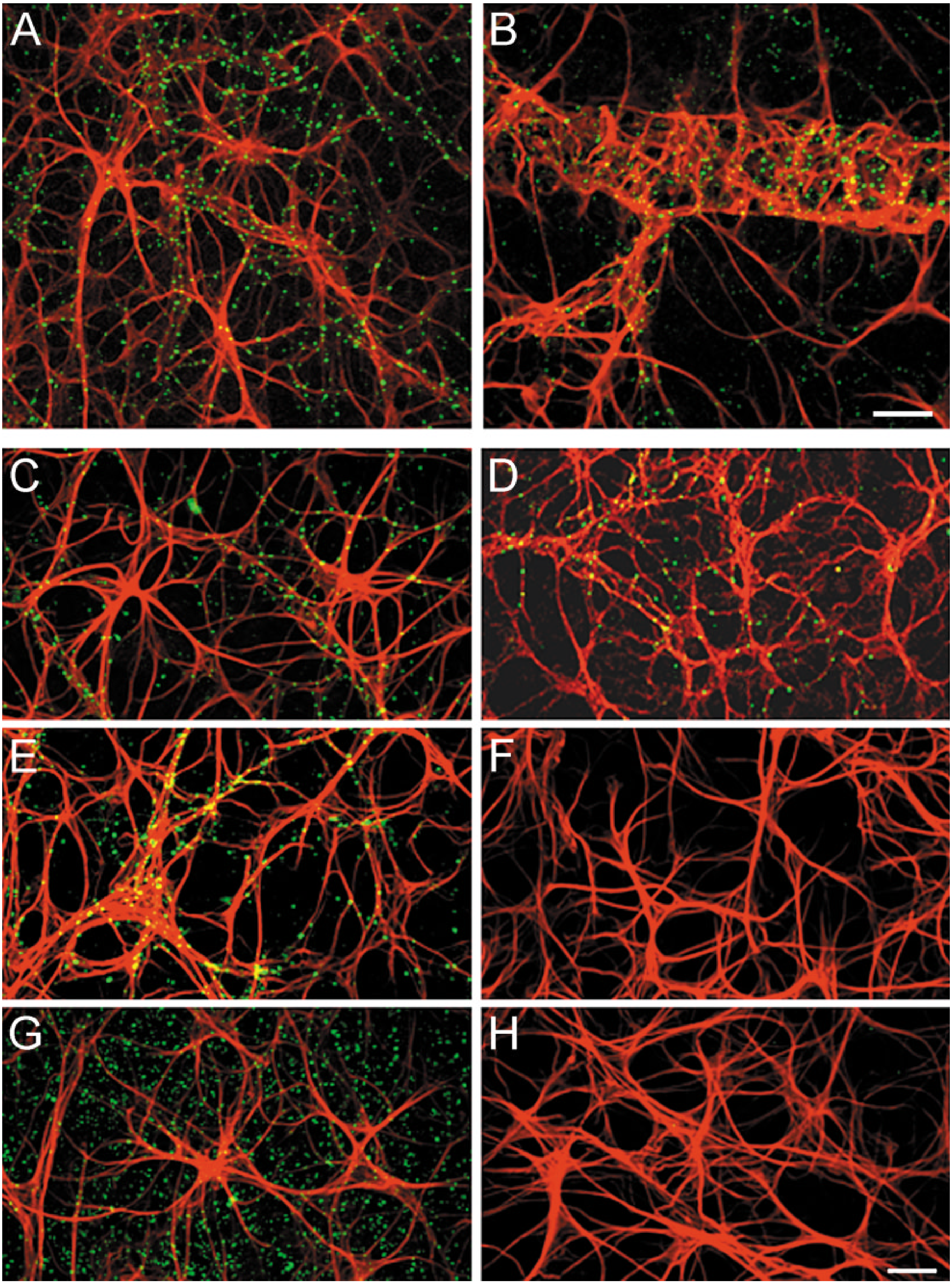

Figure 2

DISCUSSION

The purpose of this study was to identify the connexins in the rat retina that might form gap junctions between retinal glia. Immunostaining coupled with confocal microscopy allowed us to detect several connexins in the retina and to describe their laminar distribution.

Cx43

Cx43 in astrocytes. Using several different antibodies, we consistently observed that Cx43-IR puncta followed GFAP-IR astrocyte processes at the inner (vitreal) surface of the retina. These results imply that gap junctions formed by retinal astrocytes contain Cx43. The ubiquity of Cx43 in gap junctions formed by astrocytes in the brain (Dermietzel et al., 1989; Yamamoto et al., 1990a, 1991; Nagy et al., 1992, 1999; Dermietzel and Spray, 1993) and in culture (Dermietzel et al., 1991; Hofer and Dermietzel, 1998; Kunzelmann et al., 1999; Reuss et al., 2000) is well documented. Recent reports have confirmed the colocalization of Cx43 and GFAP immunoreactivity in the retinas of pigmented mice (Güldenagel et al., 2000; Söhl et al., 2000) and rabbits (Johansson et al., 1999). Cx43 immunoreactivity has also been detected at the inner limiting membrane (Janssen-Bienhold et al., 1996) and in the nerve fiber layer of the retinas of albino rats (Janssen-Bienhold et al., 1998), which is consistent with an astrocytic localization. Cx43 mRNA has been detected in the RGC and nerve fiber layers of the mouse retina, which is consistent with localization to astrocytes (Söhl et al., 2000).

Cx43 in Müller cells. Two of the antibodies used in this study (the polyclonal Zymed 71-0700, lot 90647439, and the monoclonal Zymed 13-8300) labeled profiles associated with Müller cells. This result is consistent with findings in the rabbit retina, where Cx43 is symmetrically distributed on astrocyte–astrocyte, astrocyte–Müller cell, and Müller cell–Müller cell gap junctions (Johansson et al., 1999). However, Cx43 mRNA has not been reported to be present in the INL of the mouse retina, where the Müller cell somata are located (Söhl et al., 2000). Species differences might explain the presence of Cx43 protein in rat and rabbit Müller cells and the apparent absence of Cx43 mRNA in mouse Müller cells. Alternatively, Cx43 immunoreactivity in Müller cells might reflect the internalization by Müller cells of heterotypic astrocyte–Müller cell gap junctions, in which astrocytes contribute connexons formed by Cx43 and Müller cells contribute connexons formed by a different connexin. The internalization of the entire gap junction by one cell of a coupled pair has been demonstrated (Jordan et al., 2000). Although this possibility could explain our observations at the light level in the rat retina, it is not a likely explanation for the rabbit retina, in which Cx43 labels the Müller cell sides of gap junctions studied ultrastructurally (Johansson et al., 1999). Finally, in the absence of retinas from Cx43 null mice with which to test these antibodies, we cannot rule out the possibility that the antibodies recognize species other than Cx43 in the retina. In situ hybridization studies in rat and rabbit retinas are necessary to resolve this issue.

Do the antibodies that stain astrocytes and Müller cells recognize differentially phosphorylated forms of Cx43? Although two of the anti-Cx43 antibodies used in this study labeled Müller cells throughout their length, the other four anti-Cx43 antibodies exclusively labeled profiles associated with astrocyte processes at the vitreal surface. It is possible that some of this surface connexin immunoreactivity was on the Müller cell side of astrocyte–Müller cell gap junctions, which cannot be determined at the light microscopic level. Yet the question remains as to the differences in the epitopes recognized by polyclonal Zymed 71-0700, lot 90647439, and the monoclonal Zymed 13-8300, which clearly label Müller cells, and the epitopes recognized by the other antibodies. The monoclonal antibody Zymed 13-8300 has been reported to recognize Cx43 only when it is not phosphorylated at serine 368 (Nagy et al., 1997; Cruciani and Mikalsen, 1999). Our Western blots failed to demonstrate that the antibodies that differentially stained astrocytes and Müller cells recognized differentially phosphorylated isoforms of Cx43. All of the antibodies tested stained only single bands (as opposed to doublets or triplets) of ~43 kDa in samples from brain and retina, which suggests that Cx43 in the neural tissue underwent peri-mortem dephosphorylation in our preparations. Patterns of immunostaining for Cx43 have been shown to vary with the (patho-)physiological state of astrocytes (Rohlmann et al., 1993, 1994; Hossain et al., 1994a,c; Ochalski et al., 1995; Nagy et al., 1996; Li et al., 1998; Li and Nagy, 2000), and these variations have been attributed to epitope masking (Ochalski et al., 1995). The differences in the staining patterns revealed by the different antibodies in this study imply that at least some of the Cx43 in Müller cells is in a state different from that of the Cx43 in astrocytes.

Are there gap junctions between Müller cells? The distribution of connexin immunoreactivity throughout the length of the Müller cells was somewhat surprising. We expected to observe connexin immunoreactivity associated with Müller cells in the inner retina, reflecting connexin trafficking to/from the Müller cell endfeet, where Müller cells are coupled to astrocytes (Robinson et al., 1993; Zahs and Newman, 1997). Cx43 immunoreactivity is present in the distal regions of Müller cells in fish (Giblin and Christensen, 1997; Ball and McReynolds, 1998) and amphibians (Ball and McReynolds, 1998), animals in which there are gap junctions between Müller cells (Uga and Smelser, 1973; Mobbs et al., 1988; Ball and McReynolds, 1998). It has been generally accepted that there are no gap junctions between mammalian Müller cells, but this view should be reconsidered. Although several ultrastructural

Fig. 2. Cx30 and Cx43 in retinal astrocytes. Confocal reconstructions of the surfaces of paraformaldehyde-fixed retinas doubly immunostained with antibodies directed against connexins (green) and GFAP (red). **A,B:** Cx30. A is in the peripheral retina; B is in the central retina and includes a retinal arteriole running horizontally across the upper one-third of the image. **C–H:** Cx43. Chemicon MAB3068 (C); KAαCx43 (D); and Zymed 71-0700, lot 90647439 (E) yielded punctate immunoreactivity that colocalized with GFAP-immunoreactive astrocyte processes. Two additional lots of the polyclonal anti-Cx43 (Zymed 71-0700, lots 50826441 and 80140147) yielded a pattern of staining indistinguishable from the patterns illustrated in C and D. Staining with the Zymed polyclonal antibodies was eliminated when the antibodies were preincubated with peptide antigen (F, example shown for antibody lot 90647439). However, immunostaining obtained with the monoclonal anti-connexin43 Zymed 13-8300 does *not* colocalize with GFAP-immunoreactive astrocyte processes (G), and staining is eliminated by peptide preabsorption (H). Scale bar in B = 10 μm for A,B; bar in H = 20 μm for C–H.

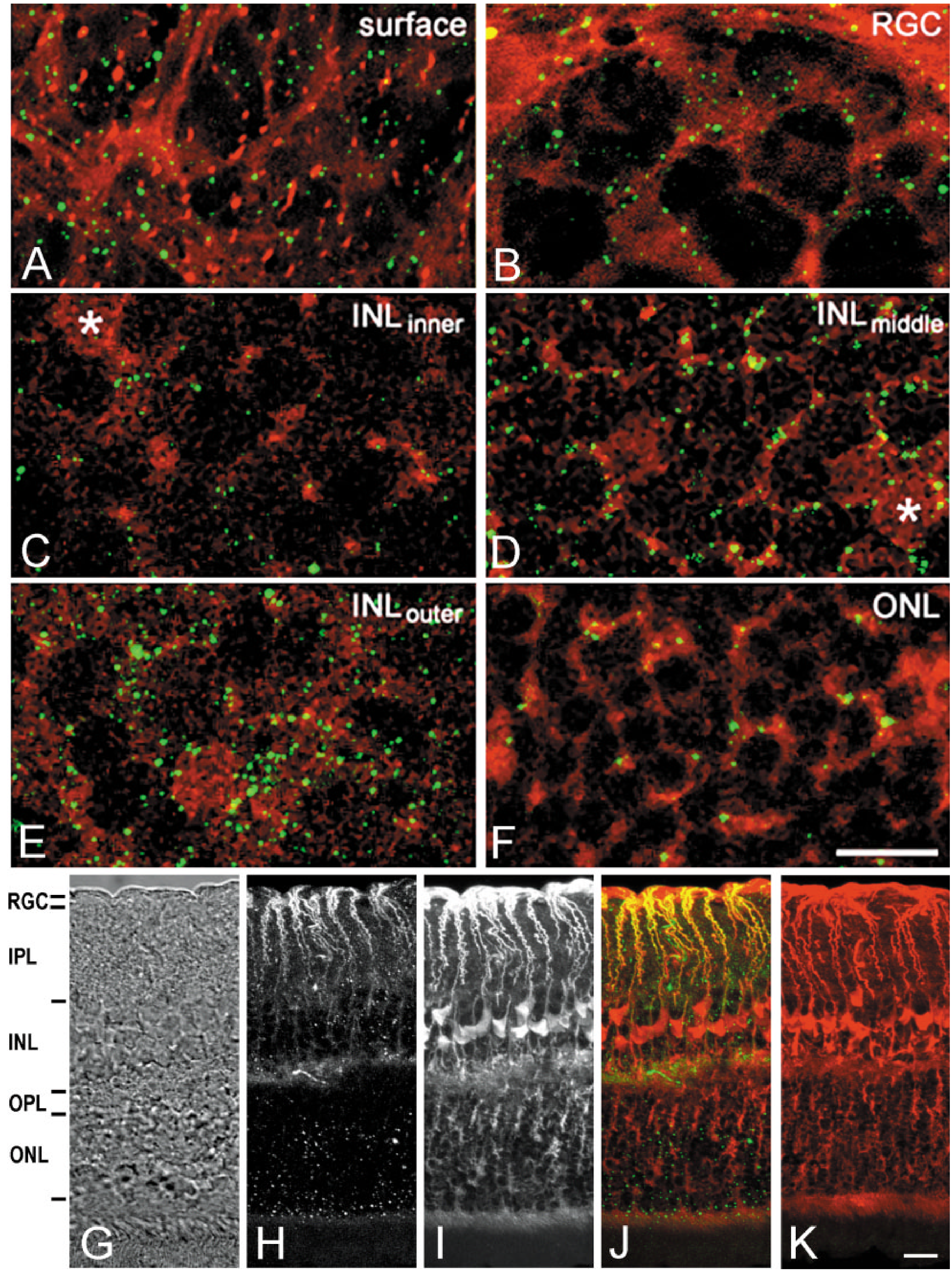
surface
A
RGC
B
*
INL inner
C
INL middle
*
D
INL outer
E
ONL
F
RGC
IPL
INL
OPL
ONL
G
H
I
J
K

Figure 3

studies failed to demonstrate gap junctions associated with mammalian Müller cells (Uga and Smelser, 1973; Bussow, 1980; Holländer et al., 1991), the demonstration of tracer coupling between astrocytes and Müller cells (Robinson et al., 1993; Zahs and Newman, 1997) refutes the conclusion that Müller cells do not participate in any gap junctions. More recently, Johansson and colleagues (1999) have demonstrated Cx43-IR gap junctions between rabbit Müller cells. Functional coupling between mammalian Müller cells has yet to be conclusively demonstrated. Results of electrical coupling experiments in the rat retina are consistent with the presence of Müller cell-to-Müller cell gap junctions, but the interpretation of these data is complicated by the presence of intervening astrocytes (Ceelen et al., 2001). In the periphery of the rabbit retina, which contains Müller cells but no astrocytes, current injections into Müller cells evoke voltage changes in neighboring Müller cells (our unpublished observations), but we have been unable to demonstrate unequivocally that this current spread is via gap junctions.

We cannot eliminate the possibility that the Cx43 in Müller cells in the outer retina is present in gap junctions between Müller cells. Another possibility is that the Cx43 immunoreactivity is present in hemichannels. There is an increasing body of evidence that connexin hemichannels may serve as pathways for the release of signaling molecules from cells, including ATP (Cotrina et al., 1998) and NAD^+ (Bruzzone et al., 2000). ATP is released during the propagation of intercellular Ca^{2+} waves between retinal glia (Newman, 2001) and NAD^+ acts extracellularly to evoke Ca^{2+} responses in Müller cells (Esguerra and Miller, 2002). It has recently been reported that current flow through Cx26 hemichannels in horizontal cells of the retina mediates feedback onto photoreceptors, providing the first example of a physiological role for hemichannels in a relatively intact tissue (Kamermans et al., 2001).

Cx30

Cx30 immunoreactivity was confined to the vitreal surface of the retina, where immunoreactive puncta colocalized with GFAP-IR astrocyte processes. Cx30 mRNA has not been detected in the mouse retina using reverse transcriptase-polymerase chain reaction (RT-PCR; Güldenagel et al., 2000). The absence of Cx30 in the mouse retina may reflect species differences between the rat and the mouse.

Cx30 has been demonstrated in astrocytes throughout the brain and spinal cord; immunoreactivity is pronounced between astrocyte endfeet abutting blood vessels (Kunzelmann et al., 1999; Nagy et al., 1999). These results are consistent with our finding that Cx30-IR puncta colocalize with GFAP-IR astrocyte processes and with our impression that these puncta are frequently located where the astrocyte processes contact the superficial retinal blood vessels. In the brain, Cx30 immunoreactivity is much greater in gray matter than in white matter tracts. Retinal astrocytes are immigrants from the optic nerve (Watanabe and Raff, 1988), yet they display robust Cx30 immunoreactivity. These findings suggest that the set of connexins expressed by astrocytes is at least partly a function of the local environment of the cells and does not depend only on cell lineage.

Cx30 immunoreactivity in brain astrocytes frequently colocalizes with Cx43 immunoreactivity, although the onset of Cx30 expression occurs after the onset of expression of Cx43 (Dahl et al., 1996; Kunzelmann et al., 1999; Nagy et al., 1999). It has been suggested that gap junctions composed of Cx30 and Cx43 may have different permeabilities to lactate or other glucose metabolites (Nagy et al., 1999) and that gap junctions composed of Cx30 may have a special role in K^+ spatial buffering (Kunzelmann et al., 1999).

Cx45

Immunoreactive puncta were observed throughout the depth of the retina with three different antibodies directed against Cx45. Cx45-IR profiles were found primarily over glutamine synthetase- or S100-IR Müller cell processes. In addition, Cx45-IR puncta were found over S100-labeled astrocyte processes, which were distinguishable from Müller cell processes by their shape and location. Cx45 mRNA has been detected in the mouse retina by RT-PCR, and a lacZ reporter gene substituted for the open reading frame of Cx45 was expressed in RGCs and somata in the INL (Güldenagel et al., 2000). Using frozen sections of the mouse retina, Güldenagel et al. also found Cx45 immunoreactivity in the inner retina as well as in the outer plexiform layer, and they concluded that Cx45 is present in amacrine cells and possibly some horizontal cells. Our observations are consistent with the expression of Cx45 by some amacrine cells. In confocal images collected parallel to the retinal layers, it is apparent that the pronounced Cx45 immunoreactivity surrounding horizontal cells is localized to the Müller cell processes surrounding these neurons (Fig. 5).

Outside of the retina, Cx45 is present in oligodendrocytes (Dermietzel et al., 1997; Kunzelmann et al., 1997). Cx45 mRNA and protein have also been detected in cultured astrocytes (Dermietzel et al., 2000b).

Potential composition of gap junctions between retinal glia

In the current study, immunoreactivity for Cx30, Cx43, and Cx45 colocalized with astrocyte markers, while immunoreactivity for Cx43 and Cx45 colocalized with Müller

Fig. 3. Monoclonal antibody 13-8300, directed against Cx43, labels Müller cells. Paraformaldehyde-fixed retina doubly immunostained using the Zymed monoclonal antibody 13-8300 (green) and polyclonal anti-S100 (red). **A–F:** Each panel represents the superimposition of six confocal images collected at 0.2 μm intervals in a plane parallel to the retinal layers. Cx43-immunoreactive puncta largely colocalize with S100-immunoreactive profiles. At the retinal surface, S100 labels astrocytes and Müller cell endfeet. Because astrocytes are located only at the vitreal surface of the retina, S100 immunoreactivity in the other retinal layers is localized in Müller cells. A: Vitreal surface. B: Müller cell processes surrounding neurons in the retinal ganglion cell (RGC) layer. Müller cell somata (asterisk) as well as processes are labeled in the inner (C), middle (D), and outer (E) portions of the inner nuclear layer (INL). F: Distal processes of Müller cells surround photoreceptor somata within the outer nuclear layer (ONL). **G–K:** Retinal sections. Retinal section (transmitted light image shown in G) doubly immunostained with Zymed monoclonal antibody 13-8300 (shown in H and in green in pseudocolor overlay in J) and S100 (shown in I and in red in pseudocolor overlay in J). K: Peptide preabsorption eliminates staining with antibody 13-8300: retinal section doubly immunostained with anti-S100 (red) and with monoclonal antibody 13-8300 that had been incubated with peptide antigen (green). The boundaries of the retinal layers are indicated. IPL, inner plexiform layer; OPL, outer plexiform layer. Scale bar in F = 10 μm for A–F; bar in K = 15 μm for G–K.

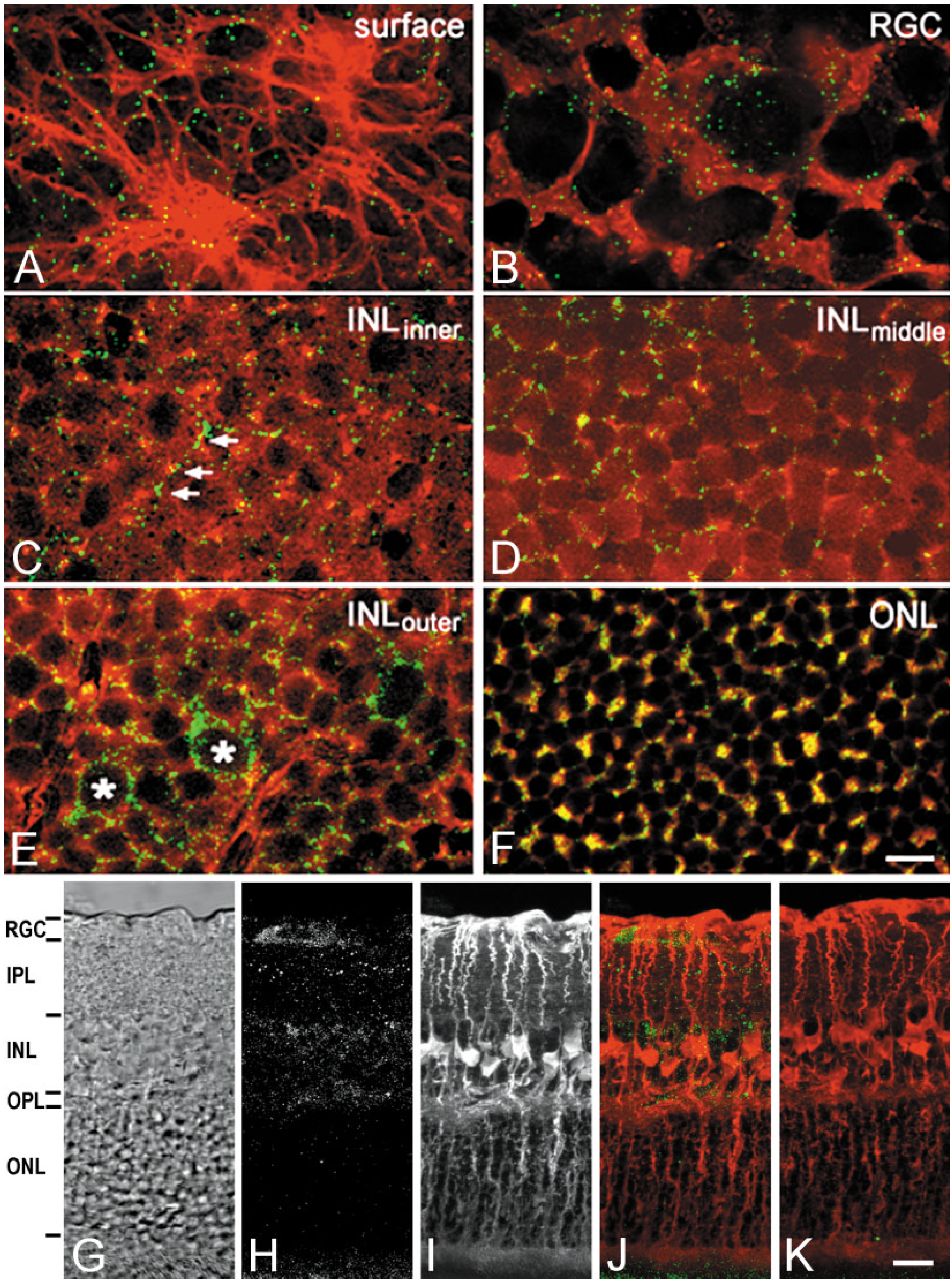
surface
A
RGC
B
INLinner
C
INLmiddle
D
INLouter
E
ONL
F
RGC
IPL
INL
OPL
ONL
G
H
I
J
K

Figure 4

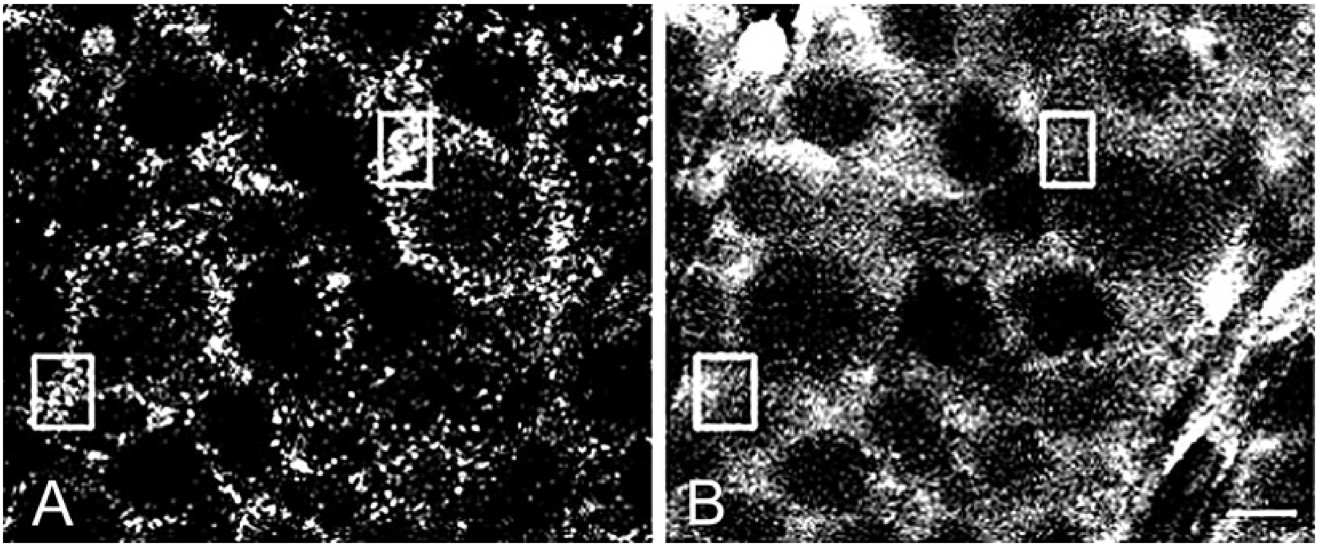

Fig. 5. Cx45 immunoreactivity in Müller cell processes that surround horizontal cells. The field shown in Figure 4E is enlarged, and the staining with the anti-Cx45 (**A**) and anti-S100 (**B**) antibodies are shown separately. Boxes are drawn around two corresponding regions in each image to facilitate comparison of the locations of the connexin staining and the S100-immunoreactive Müller cell processes. Scale bar = 5 μm.

cell markers. Several patterns of connexin expression by retinal glia could result in this pattern of immunoreactivity observed at the light microscopic level: 1) Retinal astrocytes express Cx30, Cx43, and/or Cx45, while Müller cells express Cx43 and/or Cx45. 2) One or more of the connexins that colocalize with astrocyte processes (-30, -43, -45) are actually localized to the Müller cell side of astrocyte–Müller cell gap junctions. 3) Cx43 and/or Cx45 are expressed exclusively in astrocytes in the retina, and the immunoreactivity for these connexins observed in Müller cells is due to internalization by Müller cells of heterotypic gap junctions (with Cx43 or Cx45 on the astrocyte side of the gap junction). This latter possibility seems unlikely, in that connexin immunoreactivity is observed throughout the length of the Müller cell. If this immunoreactivity is indeed present in heterotypic gap junctions that are being degraded, we would expect to have seen this immunoreactivity primarily in the inner retina, in the proximal stalks of the Müller cells. In situ hybridization studies will be necessary to localize the mRNAs for these connexins to specific cell types in the rat retina. However, based on the results presented in this study, as well as results from studies of the expression and localization of connexins in brain glia, we propose that retinal astrocytes express Cx30 and Cx43 and possibly Cx45, while Müller cells express Cx43 and Cx45. In addition, Cx50 has been localized to Müller cells and astrocytes in the retinas of albino rats (Schutte et al., 1998).

The pattern of immunoreactivity that we observe in the retina is consistent with several possible astrocyte–Müller cell gap junctions: Cx43/Cx43, Cx45/Cx45, Cx43/Cx45, and Cx45/Cx43. By including the results of Schutte et al. (1998), this list can be expanded to include the possibility of homotypic astrocyte–Müller cell gap junctions composed of Cx50. The possibility that there are heteromeric connexons in one or both cell types increases the number of potential types of gap junctions that could form between these cells.

The asymmetry of the coupling between retinal astrocytes and Müller cells (Robinson et al., 1993; Zahs and Newman, 1997) is consistent with the presence of heterotypic gap junctions between these cells (Flagg-Newton and Loewenstein, 1980). The results of ultrastructural immunohistochemical studies of brain glial cells have led several authors to suggest that astrocyte–oligodendrocyte gap junctions may be composed of Cx43/Cx45 and/or Cx30/Cx32 (Dermietzel et al., 1997; Kunzelmann et al., 1997; Li et al., 1997; Nagy et al., 1999). In addition to the expression of Cx45, Müller cells share other properties with oligodendrocytes, including the expression of carbonic anhydrase (Linser et al., 1984) and cellular retinaldehyde-binding protein (Saari et al., 1997) and a morphological relationship with retinal ganglion cell axons (Holländer et al., 1991). Considering the functional properties shared by Müller cells and oligodendrocytes, we propose that

Fig. 4. Cx45 immunoreactivity colocalizes with retinal glial cells. Paraformaldehyde-fixed retina doubly immunostained using Chemicon MAB3101 directed against Cx45 (green) and a polyclonal antibody directed against S100 (red). **A–F:** Each panel represents the superimposition of six confocal images collected at 0.2 μm intervals in a plane parallel to the retinal layers. Anti-S100 stains astrocytes at the vitreal surface (**A**) and Müller cells throughout the depth of the retina (**B–F**). Arrows in C mark a linear array of Cx45-IR puncta, which may represent staining of a neuronal process. Asterisks in E mark the somata of two presumed horizontal cells, which are surrounded by heavily Cx45-IR Müller cell (S100-IR) processes. **G–K:** Retinal sections. Retinal section (transmitted light image shown in G) doubly immunostained with MAB3101 (shown in H and in green in pseudocolor overlay in J) and S100 (shown in I and in red in pseudocolor overlay in J). K: Peptide preabsorption eliminates staining with antibody MAB3101: retinal section doubly immunostained with anti-S100 (red) and with monoclonal antibody MAB3101 that had been incubated with peptide antigen (green). Scale bar in F = 10 μm for A–F; bar in K = 15 μm for G–K.

astrocyte–Müller cell gap junctions are heterotypic channels formed by Cx43/Cx45.

The biophysical and electrophysiological properties of gap junctions composed of Cx43/Cx45 also make them likely candidates for the gap junctions between retinal astrocytes and Müller cells. Under our experimental conditions, astrocytes are ~10 mV depolarized relative to Müller cells (Zahs and Newman, 1997). The voltage gradient that would exist across astrocyte–Müller cell gap junctions could be significant if Cx45 contributes to these channels. At least in the *Xenopus* expression system, gap junctions formed by Cx45 are highly voltage-dependent: The steady-state junctional conductance is reduced to 50% of maximal levels at transjunctional voltages of ±14 mV (Steiner and Ebihara, 1996) compared with ~55 mV for Cx43 (White et al., 1994). Furthermore, heterotypic Cx43/Cx45 channels display asymmetric voltage dependences, such that hyperpolarization of the Cx45 side of the junction causes a slow inactivation of junctional current, while depolarization of the Cx45 side of the junction causes an increase in junctional current (Steiner and Ebihara, 1996). Under the conditions of our experiments, if the astrocyte–Müller cell gap junctions are indeed formed by Cx43/Cx45, we expect a significant fraction of these channels to be closed. Conditions that lead to a reduction of the voltage gradient between astrocytes and Müller cells are expected to increase the conductance of these gap junctions.

Regulation of coupling

The existence of multiple connexins within retinal glia could endow these cells with a set of diverse gap junction channels that vary in their selective permeabilities and modes of regulation. Gap junctions between astrocytes are permeable to the tracer Lucifer yellow, but gap junctions between astrocytes and Müller cells are not (Robinson et al., 1993; Zahs and Newman, 1997). Channels formed by different connexins vary in their permeabilities to biological signaling molecules, including inositol trisphosphate (Niessen et al., 2000) and nucleotides (Bevans et al., 1998; Nicholson et al., 2000). It remains to be determined how gap junctions between retinal glia differ in their permeabilities to biologically relevant molecules.

There is also little information on the regulation of gap-junctional coupling between retinal glia. Astrocyte–astrocyte gap junctions and astrocyte–Müller cell gap junctions differ in their sensitivities to pharmacological uncoupling agents (Zahs and Newman, 1997), but there are no data regarding the effects of neuromodulators or physiological conditions on coupling between retinal glia. There is extensive gap-junctional coupling between neurons in the mammalian retina, and neuronal coupling can be modulated by light exposure (Bloomfield et al., 1997; Xin and Bloomfield, 1999) and by neuromodulators (DeVries and Schwartz, 1989; Miyachi et al., 1990; Hampson et al., 1992; Mills and Massey, 1995; Weiler et al., 1999; He et al., 2000). Factors derived from the vasculature, including nitric oxide (DeVries and Schwartz, 1989; Miyachi et al., 1990; Bolanos and Medina, 1996; Yang and Hatton, 1999) and endothelin-1 (Tabernero et al., 1996), have been shown to modulate junctional coupling between cultured astrocytes, and there is circumstantial evidence that a vascular factor might differentially influence astrocyte–astrocyte and astrocyte–Müller cell coupling (Zahs and Wu, 2001).

ACKNOWLEDGMENTS

We thank Catherine Sohn and Kelsey Lessard for excellent technical assistance. We also thank Zymed Laboratories for the gift of the synthetic peptide used to generate the anti-Cx30 antibody and Chemicon International for the gift of MAB3100 and MAB3101.

LITERATURE CITED

Ball AK, McReynolds JS. 1998. Localization of gap junctions and tracer coupling in retinal Müller cells. J Comp Neurol 393:48–57.

Bevans CG, Kordel M, Rhee SK, Harris AL. 1998. Isoform composition of connexin channels determines selectivity among second messengers and uncharged molecules. J Biol Chem 273:2808–2816.

Beyer EC, Paul DL, Goodenough DA. 1987. Connexin43: a protein from rat heart homologous to a gap junction protein from liver. J Cell Biol 105:2621–2629.

Beyer EC, Paul DL, Goodenough DA. 1990. Connexin family of gap junction proteins. J Membr Biol 116:187–194.

Beyer EC, Gemel J, Seul KH, Larson DM, Banach K, Brink PR. 2000. Modulation of intercellular communication by differential regulation and heteromeric mixing of co-expressed connexins. Braz J Med Biol Res 33:391–397.

Bloomfield SA, Xin D, Osborne T. 1997. Light-induced modulation of coupling between AII amacrine cells in the rabbit retina. Vis Neurosci 14:565–576.

Bolanos JP, Medina JM. 1996. Induction of nitric oxide synthase inhibits gap junction permeability in cultured rat astrocytes. J Neurochem 66:2091–2099.

Bruzzone S, Guida L, Zocchi E, Franco L, De Flora A. 2000. Connexin 43 hemichannels mediate Ca^{2+}-regulated transmembrane NAD^{+} fluxes in intact cells. FASEB J 15:10–12.

Bussow H. 1980. The astrocytes in the retina and optic nerve head of mammals: a special glia for the ganglion cell axons. Cell Tissue Res 206:367–378.

Ceelen PW, Lockridge A, Newman EA. 2001. Electrical coupling between glial cells in the rat retina. Glia 35:1–13.

Charles AC, Naus CCG, Zhu D, Kidder GM, Dirksen ER, Sanderson MJ. 1992. Intercellular calcium signaling via gap junctions in glioma cells. J Cell Biol 118:195–201.

Charles AC, Dirksen ER, Merrill JE, Sanderson MJ. 1993. Mechanisms of intercellular calcium signaling in glial cells studied with dantrolene and thapsigargin. Glia 7:134–145.

Clark B, Mobbs P. 1994. Voltage-gated currents in rabbit retinal astrocytes. Eur J Neurosci 6:1406–1414.

Coppen SR, Dupont E, Rothery S, Severs NJ. 1998. Connexin45 expression is preferentially associated with the ventricular conduction system in mouse and rat heart. Circ Res 82:232–243.

Cotrina ML, Lin JHC, Alves-Rodrigues A, Liu S, Li J, Azmi-Ghadimi H, Kang J, Naus CCG, Nedergaard M. 1998. Connexins regulate calcium signaling by controlling ATP release. Proc Natl Acad Sci USA 95: 15735–15740.

Cruciani V, Mikalsen SO. 1999. Stimulated phosphorylation of intracellular connexin43. Exp Cell Res 251:285–298.

Dahl E, Manthey D, Schwarz H, Chang Y, Lally P, Nicholson B, Willecke K. 1996. Molecular cloning and functional expression of mouse connexin30, a gap junction gene highly expressed in adult brain and skin. J Biol Chem 271:17903–17910.

Dermietzel R, Spray DC. 1993. Gap junctions in the brain: where, what type, how many and why? Trends Neurosci 16:186–192.

Dermietzel R, Traub O, Hwang TK, Beyer E, Bennett MVL, Spray DC, Willecke K. 1989. Differential expression of three gap junction proteins in developing and mature brain tissues. Proc Natl Acad Sci USA 86:10148–10152.

Dermietzel R, Hertzberg EL, Kessler JA, Spray DC. 1991. Gap junctions between cultured astrocytes: immunocytochemical, molecular, and electrophysiological analysis. J Neurosci 11:1421–1432.

Dermietzel R, Farooq M, Kessler JA, Althaus H, Hertzberg EL, Spray DC. 1997. Oligodendrocytes express gap junction proteins connexin32 and connexin45. Glia 20:101–114.

Dermietzel R, Kremer M, Paputsoglu G, Stang A, Skerett IM, Gomès D, Srinivas M, Janssen-Bienhold U, Weiler R, Nicholson BJ, Bruzzone R, Spray DC. 2000a. Molecular and functional diversity of neuronal connexins in the retina. J Neurosci 15: 8331–8343.

Dermietzel R, Gao Y, Scemes E, Viera D, Urban M, Kremer M, Bennett MV, Spray DC. 2000b. Connexin43 null mice reveal that astrocytes express multiple connexins. Brain Res Brain Res Rev 32:45–56.

DeVries SH, Schwartz EA. 1989. Modulation of an electrical synapse between solitary pairs of catfish horizontal cells by dopamine and second messengers. J Physiol 414:351–375.

Esguerra M, Miller RF. 2002. CD38 expression and NAD^+-induced intracellular Ca^{2+} mobilization in isolated retinal Muller cells. Glia 39: 314–319.

Flagg-Newton JL, Loewenstein WR. 1980. Asymmetrically permeable membrane channels in cell junctions. Science 207:771–773.

Giaume C, Fromaget C, El Aoumari A, Cordier J, Glowinski J, Gros D. 1991. Gap junctions in cultured astrocytes: single-channel currents and characterization of channel-forming protein. Neuron 6:133–143.

Giaume C, Tabernero A, Medina JM. 1997. Metabolic trafficking through astrocytic gap junctions. Glia 21:114–123.

Giblin LJ, Christensen BN. 1997. Connexin43 immunoreactivity in the catfish retina. Brain Res 755:146–150.

Güldenagel M, Söhl G, Plum A, Traub O, Teubner B, Weiler R, Willecke K. 2000. Expression patterns of connexin genes in mouse retina. J Comp Neurol 425:193–201.

Hampson EC, Vaney DI, Weiler R. 1992. Dopaminergic modulation of gap junction permeability between amacrine cells in mammalian retina. J Neurosci 12:4911–4922.

He S, Weiler R, Vaney DI. 2000. Endogenous dopaminergic regulation of horizontal cell coupling in the mammalian retina. J Comp Neurol 418:33–40.

Hofer A, Dermietzel R. 1998. Visualization and functional blocking of gap junction hemichannels (connexons) with antibodies against external loop domains in astrocytes. Glia 24:141–154.

Holländer H, Makarov F, Dreher Z, Driel DV, Chan-Ling T, Stone J. 1991. Structure of the macroglia of the retina: sharing and division of labour between astrocytes and Müller cells. J Comp Neurol 313:587–603.

Hossain M, Peeling J, Sutherland G, Hertzberg EL, Nagy JI. 1994a. Ischemia-induced cellular redistribution of the astrocytic gap junctional protein connexin43 in rat brain. Brain Res 652:311–322.

Hossain MZ, Murphy LJ, Hertzberg EL. 1994b. Phosphorylated forms of connexin43 predominate in rat brain: demonstration by rapid inactivation of brain metabolism. J Neurochem 62:2349–2403.

Hossain MZ, Sawchuk MA, Murphy LJ, Hertzberg EL, Nagy JI. 1994c. Kainic acid induced alterations in antibody recognition of connexin43 and loss of astrocytic gap junctions in rat brain. Glia 10:250–265.

Janssen-Bienhold U, Dermietzel R, Weiler R. 1996. Distribution of connexin43 immunoreactivity in the retinas of different vertebrates. Soc Neurosci Abstr 22:822.

Janssen-Bienhold U, Dermietzel R, Weiler R. 1998. Distribution of connexin43 immunoreactivity in the retinas of different vertebrates. J Comp Neurol 396:310–321.

Johansson K, Bruun A, Ehinger B. 1999. Gap junction protein connexin43 is heterogeneously expressed among glial cells in the adult rabbit retina. J Comp Neurol 407:395–403.

Jones PS, Elias JM, Schecter N. 1986. An improved method for embedding retina for cryosectioning. J Histotech 9:181–182.

Jordan K, Chodock R, Hand AR, Laird DW. 2000. The origin of annular junctions: a mechanism of gap junction internalization. J Cell Sci 114:763–773.

Kamermans M, Fahrenfort I, Schultz K, Janssen-Bienhold U, Sjoerdsma T, Weiler R. 2001. Hemichannel-mediated inhibition in the outer retina. Science 292:1178–1180.

Kumai M, Nishii K, Nakamura K, Takeda N, Suzuki M, Shibata Y. 2000. Loss of connexin45 causes a cushion defect in early cardiogenesis. Development 127:3501–3512.

Kumar NM. 1999. Molecular biology of the interactions between connexins. Novartis Found Symp 219:6–16.

Kunzelmann P, Blumcke I, Traub O, Dermietzel R, Willecke K. 1997. Coexpression of connexin45 and -32 in oligodendrocytes of rat brain. J Neurocytol 26:17–22.

Kunzelmann P, Schroder W, Traub O, Steinhauser C, Dermietzel R, Willecke K. 1999. Late onset and increasing expression of the gap junction protein connexin30 in adult murine brain and long-term cultured astrocytes. Glia 25:111–119.

Laird DW, Puranam KL, Revel JP. 1991. Turnover and phosphorylation dynamics of connexin43 gap junction protein in cultured cardiac myocytes. Biochem J 273:67–72.

Lee SH, Kim WT, Cornell-Bell AH, Sontheimer H. 1994. Astrocytes exhibit regional specificity in gap junction coupling. Glia 11:315–325.

Li J, Hertzberg EL, Nagy JI. 1997. Connexin 32 in oligodendrocytes and association with myelinated fibers in mouse and rat brain. J Comp Neurol 379:571–591.

Li WEI, Nagy JI. 2000. Activation of fibres in rat sciatic nerve alters phosphorylation state of connexin-43 at astrocytic gap junctions in spinal cord: evidence for junction regulation by neuronal–glial interactions. Neuroscience 97:113–123.

Li WEI, Ochalski PAY, Hertzberg EL, Nagy JI. 1998. Immunorecognition, ultrastructure and phosphorylation status of astrocytic gap junctions and connexin43 in rat brain after cerebral focal ischaemia. Eur J Neurosci 10:2444–2463.

Linser PJ, Sorrentino M, Moscona AA. 1984. Cellular compartmentalization of carbonic anhydrase-C and glutamine synthetase in developing and mature mouse neural retina. Brain Res 315:65–71.

Manjunath CK, Nicholson BJ, Teplow D, Hood L, Page E, Revel J-P. 1987. The cardiac gap junction protein Mr 47,000 has a tissue-specific cytoplasmic domain of Mr 17,000 at its carboxy terminus. Biochem Biophys Res Commun 142:228–234.

Meier C, Petrasch-Parwez E, Habbes HW, Teubner B, Güldenagel M, Degen J, Söhl G, Willecke K, Dermietzel R. 2002. Immunohistochemical detection of the neuronal connexin36 in the mouse central nervous system in comparison to connexin36 deficient tissues. Histochem Cell Biol 117:461–71.

Mills SL, Massey SC. 1995. Differential properties of two gap junctional pathways made by AII amacrine cells. Nature 377:734–737.

Miyachi E, Murakami M, Nakaki T. 1990. Arginine blocks gap junctions between retinal horizontal cells. Neuroreport 1:107–110.

Mobbs P, Brew H, Attwell D. 1988. A quantitative analysis of glial cell coupling in the retina of the axolotl (*Ambystoma mexicanum*). Brain Res 460:235–245.

Musil LS, Goodenough DA. 1991. Biochemical analysis of connexin43 intracellular transport, phosphorylation, and assembly into gap junctional plaques. J Cell Biol 115: 1357–1374.

Nagy JI, Yamamoto T, Sawchuk MA, Nance DM, Hertzberg EL. 1992. Quantitative immunohistochemical and biochemical correlates of connexin43 localization in rat brain. Glia 5:1–9.

Nagy JI, Li WEI, Doble BW, Hochman S, Hertzberg EL, Kardami E. 1996. Detection of dephosphorylated Cx43 in brain, heart and in spinal cord after nerve stimulation. Soc Neurosci Abstr 22:1023.

Nagy JI, Li WEI, Roy C, Doble BW, Gilchrist JS, Kardami E, Hertzberg EL. 1997. Selective monoclonal antibody recognition and cellular localization of an unphosphorylated form of connexin43. Exp Cell Res 236: 127–136.

Nagy JI, Patel D, Ochalski PAY, Stelmack GL. 1999. Connexin30 in rodent, cat, and human brain: selective expression in gray matter astrocytes, co-localization with connexin43 at gap junctions and late developmental appearance. Neuroscience 88:447–468.

Nelles E, Bützler C, Jung D, Temme A, Gabriel H-D, Dahl U, Traub O, Stümpel F, Jungermann K, Zielasek J, Toyka KV, Dermietzel R, Willecke K. 1996. Defective propagation of signals generated by sympathetic nerve stimulation in the liver of connexin32-deficient mice. Proc Natl Acad Sci USA 93:9565–9570.

Newman EA. 2001. Propagation of intercellular calcium waves in retinal astrocytes and Müller cells. J Neurosci 21:2215–2223.

Newman EA, Reichenbach A. 1996. The Müller cell: a functional element of the retina. Trends Neurosci 19:307–312.

Nicholson BJ, Weber PA, Cao F, Chang H-C, Lampe P, Goldberg G. 2000. The molecular basis of selective permeability of connexins is complex and includes both size and charge. Braz J Med Biol Res 33:369–378.

Niessen H, Harz H, Bender P, Kramer K, Willecke K. 2000. Selective permeability of different connexin channels to the second messenger inositol 1,4,5-trisphosphate. J Cell Sci 113:1365–1372.

Ochalski PA, Sawchuk MA, Hertzberg EL, Nagy JI. 1995. Astrocytic gap junction removal, connexin43 redistribution, and epitope masking at excitatory amino acid lesion sites in rat brain. Glia 14:279–294.

Ochalski PA, Frankenstein U, Hertzberg EL, Nagy JI. 1997. Connexin-43 in rat spinal cord: localization on astrocytes and identification of heterotypic astro–oligodendrocytic gap junctions. Neuroscience 76:931–945.

Ransom BR. 1995. Gap junctions. In: Kettenmann H, Ransom BR, editors. Neuroglia. New York: Oxford University Press. p 299–318.

Ransom BR, Kettenmann H. 1990. Electrical coupling, without dye coupling, between mammalian astrocytes and oligodendrocytes in cell culture. Glia 3:258–266.

Reaume AG, de Sousa PA, Kulkarni S, Langille BL, Zhu D, Davies TC, Juneja SC, Kidder GM, Rossant J. 1995. Cardiac malformation in neonatal mice lacking connexin43. Science 267:1831–1834.

Reichenbach A, Robinson SR. 1995. Ependymoglia and ependymoglia-like cells. In: Kettenmann H, Ransom BR, editors. Neuroglia. New York: Oxford University Press. p 58–84.

Reuss B, Hertel M, Werner S, Unsicker K. 2000. Fibroblast growth factors-5 and -9 distinctly regulate expression and function of the gap junction protein connexin43 in cultured astroglial cells from different brain regions. Glia 30:231–241.

Robinson SR, Hampson ECGM, Munro MN, Vaney DI. 1993. Unidirectional coupling of gap junctions between neuroglia. Science 262:1072–1074.

Rohlmann A, Laskawi R, Hofer A, Dobo E, Dermietzel R, Wolff JR. 1993. Facial nerve lesions lead to increased immunostaining of the astrocytic gap junction protein (connexin 43) in the corresponding facial nucleus of rats. Neurosci Lett 154:206–208.

Rohlmann A, Laskawi R, Hofer A, Dermietzel R, Wolff JR. 1994. Astrocytes as rapid sensors of peripheral axotomy in the facial nucleus of rats. Neuroreport 5:409–412.

Saari JC, Huang JM, Possin DE, Fariss RN, Leonard J, Garwin GG, Crabb JW, Milam AH. 1997. Cellular retinaldehyde-binding protein is expressed by oligodendrocytes in optic nerve and brain. Glia 21:259–268.

Schutte M, Chen S, Buku A, Wolosin J. 1998. Connexin50, a gap junction protein of macroglia in the mammalian retina and visual pathway. Exp Eye Res 66:605–613.

Shashoua VE, Hesse GW, Moore BW. 1984. Proteins of the brain extracellular fluid: evidence for release of S-100 protein. J Neurochem 42: 1536–1541.

Söhl G, Güldenagel M, Traub O, Willecke K. 2000. Connexin expression in the retina. Brain Res Brain Res Rev 32:138–145.

Spray D, Moreno AL, Kessler J, Dermietzel R. 1991. Characterization of gap junctions between cultured leptomeningeal cells. Brain Res 568:1–14.

Steiner E, Ebihara L. 1996. Functional characterization of canine connexin45. J Membr Biol 150:153–161.

Tabernero A, Giaume C, Medina JM. 1996. Endothelin-1 regulates glucose utilization in cultured astrocytes by controlling intercellular communication through gap junctions. Glia 16:187–195.

Tani E, Nishiura M, Higashi M. 1973. Freeze-fracture studies of gap junctions of normal and neoplastic astrocytes. Acta Neuropathol 26: 127–138.

Uga S, Smelser GK. 1973. Comparative study of the fine structure of retinal Müller cells in various vertebrates. Invest Ophthalmol Vis Sci 12:434–448.

Van Eldik LJ, Zimmer DB. 1987. Secretion of S-100 from rat C6 glioma cells. Brain Res 436:367–370.

Watanabe T, Raff MC. 1988. Retinal astrocytes are immigrants from the optic nerve. Nature 332:834–837.

Weiler R, He S, Vaney DI. 1999. Retinoic acid modulates gap junctional permeability between horizontal cells of the mammalian retina. Eur J Neurosci 11:3346–3350.

White TW, Bruzzone R. 2000. Intercellular communication in the eye: clarifying the need for connexin diversity. Brain Res Brain Res Rev 32:130–137.

White TW, Bruzzone R, Wolfram S, Paul DL, Goodenough DA. 1994. Selective interactions among the multiple connexin proteins expressed in the vertebrate lens: the second extracellular domain is a determinant of compatibility between connexins. J Cell Biol 125:879–892.

Xin D, Bloomfield SA. 1999. Dark- and light-induced changes in coupling between horizontal cells in mammalian retina. J Comp Neurol 405:75–87.

Yamamoto T, Ochalski P, Hertzberg EL, Nagy JI. 1990a. LM and EM immunolocalization of the gap junctional protein connexin 43 in rat brain. Brain Res 508:313–319.

Yamamoto T, Ochalski P, Hertzberg EL, Nagy JI. 1990b. On the organization of astrocytic gap junctions in rat brain as suggested by LM and EM immunohistochemistry of connexin43 expression. J Comp Neurol 302:853–883.

Yamamoto T, Kardami E, Nagy JI. 1991. Basic fibroblast growth factor in rat brain: localization to glial gap junctions correlates with connexin43 distribution. Brain Res 554:336–343.

Yang QZ, Hatton GI. 1999. Nitric oxide via cGMP-dependent mechanisms increases dye coupling and excitability of rat supraoptic nucleus neurons. J Neurosci 19:4270–4279.

Zahs KR, Newman EA. 1997. Asymmetric gap junctional coupling between glial cells in the rat retina. Glia 20:10–22.

Zahs KR, Wu T. 2001. Confocal microscopic study of glial–vascular relationships in the retinas of pigmented rats. J Comp Neurol 429:253–269.